Upon impact: the fate of adhering *Pseudomonas fluorescens* cells during Nanofiltration

Olivier Habimana[1], *Andrea J.C. Semião*[2], *Eoin Casey*[1*]

Total: 4774 words, 5 figures and 3 tables

1. School of Chemical and Bioprocess Engineering, University College Dublin (UCD), IRELAND

2. School of Engineering, University of Edinburgh, Edinburgh EH9 3JL, UK

*Corresponding author. Mailing address: University College Dublin, School of Chemical and Bioprocess Engineering, Belfield, Dublin 4, IRELAND. Phone: +353 1 716 1877.

Email: eoin.casey@ucd.ie

KEYWORDS: Bacterial adhesion, Nanofiltration, permeate flux, hydrodynamic shear, cell fate

Abstract

Nanofiltration (NF) is a high pressure membrane filtration process increasingly applied in drinking water treatment and water reuse processes. NF typically rejects divalent salts, organic matter and micropollutants. However, the efficiency of NF is adversely affected by membrane biofouling, during which microorganisms adhere to the membrane and proliferate to create a biofilm. Here we show that adhered *Pseudomonas fluorescens* cells under high permeate flux conditions are met with high fluid shear and convective fluxes at the membrane-liquid interface, resulting in their structural damage and collapse. These results were confirmed by fluorescent staining, flow cytometry and scanning electron microscopy. This present study offers a "first-glimpse" of cell damage and death during the initial phases of bacterial adhesion to NF membranes, and raises a key question about the role of this observed phenomena during early stage biofilm formation under permeate flux and cross flow conditions.

Introduction

Nanofiltration (NF) is increasingly used as a polishing step in water treatment processes in order to remove organic matter and trace contaminants for the production of potable water [1]. The efficiency of NF processes is however adversely affected by the formation of a biofilm on the membrane surface[2-4]. These biofilms comprise a community of dead and viable microorganisms embedded in a matrix consisting of polysaccharides, lipids, proteins, organic matter, amongst other components [4]. Biofilms are difficult to remove and negatively impact the NF process[5-9] by decreasing permeate flux, solute retention and membrane life[10, 11]. As such, most scientific studies in the context of NF operations have predominantly focused on the mature biofilm stage.

Biofilm formation on membranes is initiated by the irreversible adhesion of bacterial cells onto the surface. Adhesion is influenced by several factors, principally, the properties of the micro-organisms, membrane characteristics, feedwater and the conditions under which the process is operated[12-17]. Initial colonization of a surface is the first step in biofilm formation[18] and an understanding of its mechanisms under representative NF operating conditions is important in order to develop new membranes, avoid the formation of biofilm and/or develop more efficient biofouling control strategies.

Despite some studies covering initial adhesion onto commercial and novel NF and RO membrane surfaces, there is a gap in the understanding of how initial adhesion is impacted by permeate flux as most studies are carried out in the absence of, or under low pressure conditions and low Reynolds numbers[14, 15, 19-21]. In contrast, the mature biofilm on NF and RO membranes has been studied under higher permeability conditions and Reynolds numbers[22-24].

Understanding bacterial-membrane interactions in NF processes representative of full-scale systems is an area of research that has not yet received priority but is nevertheless critical in order to fully understand several important aspects of NF biofouling. One such aspect involves the investigation of the physiological state of adhered cells. Some NF and RO studies have reported a biofilm layer with a high ratio of dead cells (>50%) covering the membrane surface[11, 22], whilst others have reported the quasi-absence of dead cells[24]. Finally, interspersed viable and non-viable cells along the membrane modules have also been obtained during membrane autopsy[25]. Although most studies focus on mature biofilms on NF membranes, very few have investigated the fate of bacterial cells during the initial stages of biofilm formation under conditions representative of full-scale NF processes.

The objective of this study was to investigate the effects of permeate flux and flow shear conditions on adhered *Pseudomonas fluorescens* cells using two commercial NF membranes and different membrane configurations.

Materials and Methods

Bacteria Strain and culture condition

The selected model bacterial strain for this study was an mCherry-expressing *Pseudomonas fluorescens* PCL1701 [26], stored at -80°C in King B broth [27] supplemented with 20% glycerol. Cultures were obtained by inoculating 100 mL King B broth supplemented with gentamicin at a final concentration of 10 µg mL^{-1} using a single colony of a previously grown culture on King B agar (Sigma Aldrich, Ireland) at 28°C. The inoculated medium was then incubated at 28°C with shaking at 75 rpm and left to grow to an Optical Density (OD_{600}) of 1.0.

Cell preparation for adhesion assay

To evaluate bacterial adhesion under different flux conditions, cell concentration was standardized for each adhesion experiment by diluting the growth cultures to an OD_{600} of 0.2 in 200 mL of 0.1 M NaCl (Sigma-Aldrich, Ireland). Cells were then harvested by centrifugation at a G-force corresponding to 4461.1 g for 10 min using a Sorval RC5C Plus centrifuge (Unitech, Ireland) and a FiberliteTM f10-6x500y fixed angle rotor (Thermo Fisher Scientific Inc., Dublin, Ireland), then washed twice using 0.1 M NaCl and re-suspended in 200 mL 0.1 M NaCl solution, resulting in an inoculum of approximately 10^8 cells/mL.

When needed, cells were directly adjusted to an OD_{600} of 0.2 in 200 mL of 0.1 M NaCl from an overnight culture without washing, followed by a second 1/10 dilution in a final volume 250 mL of 0.1M NaCl feed solution prior to adhesion assays.

Membranes and filtration test units

Adhesion experiments were performed on several nanofiltration and reverse osmosis membranes: NF90, NF270, BW30 and BW30 FR (Dow Filmtec Corp, USA) and ESNA1-LF and ESNA1-LF2 from Hydranautics (Nitto Denko Corp, USA). Membrane properties can be found in Table 1. Prior to adhesion experiments, membranes were cut, thoroughly rinsed with pure water and left soaking overnight in the fridge at 4°C. Adhesion experiments were carried out in cross-flow for all the membranes and in dead-end filtration for the NF90 and NF270 membranes. No feed spacers were used throughout this study.

Table 1 – NF and RO membrane properties

	Permeability (L/h.m2.bar)[a]	NaCl Retention[b] (%)
NF90	6.8±0.5	87.8±4.0
NF270	12.6±1.2	16.0±0.3
BW30	2.6±0.3	93.5±2.1
BW30 FR	2.8±0.5	92.9±1.3
ESNA 1- LF	3.5±0.4	88.8±1.5
ESNA1 - LF2	6.8±0.8	75.2±0.2

[a] Permeability measured with MilliQ water at 21°C
[b] 0.1 M NaCl at 15 bar, 21ºC and Re=579

Cross-flow system

The cross-flow system was setup as previously described[28] with a few modifications (Cf. Supplementary Information; S1). Briefly, the system was designed as a loop arrangement composed of two feed tanks, a pump, and an array of three Membrane Fouling Simulator devices (MFS) positioned in parallel working in full recirculation mode. Membranes were first placed in MFS devices and compacted for a minimum of 18 hours at 21°C with MilliQ water (18.2 MΩ.cm^{-1}, Veolia, Ireland). Pure water flux was measured for each membrane at 15 bar and at the pressure

subsequently used during the experiment. Prior to adhesion experiments, both feed tanks were filled with 4 L of a 0.1 M NaCl solution each, and bubbles were purged from the cross-flow system by recirculating the feed solution from one tank to another by coordinating the opening and closing of a system of ball valves, and ended by safely blocking one of the two feed tanks. The solution was then recirculated in the system at cross-flow experimental conditions set to 0.66 $L.min^{-1}$ or Re=579 in each cell. Three different selected pressures were tested independently, namely 3.1, 11.3 and 15.5 bar at 21°C. Both feed and permeate were recirculated back to the feed tank. During this time, permeate flux, feed and permeate conductivity were measured for each MFS. The prepared bacterial cell inoculum containing approximately 10^8 cells/mL was then added to the active feed tank and recirculated in the system at a final concentration of 10^7 cells/mL at the set filtration conditions without stopping the cross-flow system.

The concentration polarisation modulus $\beta=C_m/C_f$ was calculated after 30 minutes of adhesion based on the equation:

$$\frac{C_m - C_p}{C_f - C_p} = exp\left(\frac{J_P}{k}\right) \quad (1)$$

Where C_m, C_p and C_f are the NaCl concentrations at the membrane surface, permeate and feed, respectively, Jp is the permeate flux (m/s) and k is the mass transfer coefficient (m/s). The mass transfer coefficient was calculated as previously described by Semião et al.[29].

After 30 minutes, a non-recirculating system rinse was carried out, by first unblocking the unused feed tank containing 0.1 M NaCl and then by blocking the feed tank containing bacterial cells. This allowed flushing the system with a 0.1 M NaCl solution, allowing for the removal of non-adhered bacteria from the membrane surface while maintaining the filtration conditions. Adhesion tests for each membrane at different permeate flux conditions were repeated in at least two independent experiments.

Dead-end system

Laboratory scale dead-end filtration was carried out in a MET-cell (Membrane Extraction Technology Ltd, London, UK) composed of a stainless steel cylindrical solution chamber with a capacity of 300 mL, and fitted with a membrane porous support plate onto which the membrane was placed. A stirrer with a radius of 1.25 cm, attached to the cylinders inlet hatch was activated by placing the sealed cylinder on top of a magnetic stirrer. The cylinder was also fitted with an exit port from which the permeate was collected. A 2 L stainless steel tank was connected to the cylinder inlet port and was pressurized using a compressed nitrogen source, allowing a total feed volume of up to 2.3 L. Prior to experimentation, the working bacterial concentration in the dead-end system was adjusted to approximately 10^7 cells/mL. The experimental conditions were set at 3.1 and 15.5 bar at 21°C for a total period of 10, 15 or 30 minutes and a stirring speed of 600 rpm to avoid concentration polarisation. During this time, permeate flux and permeate conductivity were measured. At the end of the experiment the feed conductivity was also measured. For each time point, the adhesion was stopped by gradually depressurising the cylinder. Adhesion was repeated in at least three independent experiments for each membrane, set pressure and time point.

The polarisation modulus β was calculated with equation (1), where the mass transfer coefficient was calculated based on the equation in Bowen et al. [30]

Adhesion quantification and cell structural integrity evaluation

The quantification of bacterial adhesion was performed *ex-situ* for cross-flow and dead-end filtration processes. Both MFS and dead-end devices were carefully opened whilst submerged in a 0.1 M NaCl solution bath. It was previously determined that this process does not affect the adhesion of bacterial cells by more than 3% compared to doing the analysis *in-situ* (data not shown). The membranes were removed from the devices and biopsy samples were cut and placed at the bottom

of mini petri dishes whilst still submerged under 0.1 M NaCl bath. For assessing the degree of cell structural damage, fouled membranes were stained by adding and mixing 1 µL SYTOX Green ® (5 mM) (Invitrogen, Dublin, Ireland) to individual petri dishes each containing a membrane sample. Although prone to artefacts (including false staining of live cells or incomplete staining penetration), differential membrane permeability staining techniques involving dyes such as SYTOX Green ®, are by far one of the simplest ways of localizing cell-membrane integrity at the single-cell level. Monitoring changes in damaged cell ratio during our experiments allowed monitoring the level of cell fitness as a consequence of changes in permeate flux conditions. The use of SYTOX Green ® was therefore ideal for providing a reliable means of directly assessing and quantifying the degree of cell damage in the present experimental setup. Stained samples were subsequently incubated at ambient temperature for 10 minutes in the dark prior to epi-fluorescence microscopy (Olympus BX51) using a 10X objective. Two images were acquired for every chosen observation field using U-MNG and U-MWB filter cubes for differentiating between fluorescent mCherry-tagged and SYTOX Green -stained *Pseudomonas* cells, respectively. Ten different fields of view were obtained at random points from each membrane sample. Cell surface coverage (%) for mCherry-tagged and SYTOX Green -stained cells was determined for each tested membrane using ImageJ® software, a Java-based image processing program (http://rsbweb.nih.gov/ij/).

Flow cytometry

To further assess the structural integrity of bacterial cells following exposure to both high ionic strength environments and convective flux at high pressures, bacterial sampling was performed following dead-end filtration on NF 270 membranes at 15 bar for 15 minutes using a non-washed cell suspension as stated above in the “dead-end system” description. After the adhesion experiment, non-deposited *Pseudomonas* cells in the feed solution were first sampled by collecting 1 mL retentate into Eppendorf tubes. Following the careful removal of the fouled NF270 membrane

from the cylinder, a membrane sample of approximately 30 cm^2 was cut and placed in a separate Petri-dish whilst still submerged under 0.1 M NaCl. Adhered cells were then re-suspended by gently tapping and scrapping on the membrane surface using a plastic spreader, before collecting 1 mL samples into Eppendorf tubes. As a control, 1 mL of the feed bacterial suspension was collected prior to adhesion experiments in Eppendorf tubes. For assessing cell damage, bacterial samples were stained with SYTOX Green ® by adding 0.5 µL to individual Eppendorf tubes before incubation at ambient temperature in the dark for 10 minutes. Expression profiles for mCherry and SYTOX Green ® of all samples were identified and sorted by fluorescent-activated cell sorting (FACS) (BD FACSAria III Cell Sorter) using two lasers, 488 nm (blue) and 561 nm (green), with emission signals filtered through 530/30 nm and 6110/20 nm emission filters, respectively. FAC analysis was performed on at least 2 independent adhesion samples. All samples were analyzed on a FACSAria III using FlowJo software. Statistical significance of differences in gated population frequencies (%) was tested using ANOVA in MINITAB v15.1 (Minitab Inc., State College, PA, USA). The change in frequency counts in all gated populations as a result of dead-end filtration in the bulk liquid and on the membrane surface was analyzed with Tukey's test for pair wise comparisons (Minitab). All tests were performed at 5% significance level.

SEM

For scanning electron microscopy (SEM) observations, NF 270 fouled membranes following dead-end filtration at 15 bar for 15 minutes were chemically fixated and dehydrated in individual mini-Petri dishes. Submerged membrane samples were fixed by adding glutaraldehyde to a final concentration of 2.5%, and left to incubate overnight.

Separately, FACS collected sorted cells were filtered through individual 0.2 µm pore-size polycarbonate filters, which were placed in individual petri dishes and fixed overnight using a solution containing 2.5% glutaraldehyde and 0.1 M sodium cacodylate. All samples were then rinsed

with MilliQ and dehydrated in ethanol. When required, samples were exposed to 50% then 100% hexamethyldisilizane before drying in air. Samples were gold sputtered using an Eintech K575K coater for 30 s at x V 30 mA. High magnification imaging of the membrane surfaces was performed under a Hitachi Quanta 3D FEG scanning electron microscope at the UCD Nano-imaging and Materials Analysis Centre.

Results and Discussion

Effect of permeate flux on the structural integrity of Pseudomonas fluorescens cells during Nanofiltration and Reverse Osmosis

The effect of permeate flux on damaged cells to live cells ratio based on acquired SYTOX Green and mCherry positive signals of adhered *Pseudomonas fluorescens* cells to six nanofiltration and reverse osmosis membranes is shown in Figure 1. A clear positive correlation between the ratio of damaged cells and permeate flux was obtained for all tested Nanofiltration and Reverse Osmosis membranes, whereby increasing permeate flux conditions led to higher ratios of damaged adhered *P. fluorescens* cells. The only exception was the BW30 FR membrane, where the ratio did not change substantially for different permeate fluxes.

Comparatively low increases in damaged cell ratios were observed for membranes with low to mid permeate fluxes acquired at 3, 11 and 15 bar pressure filtration settings (<45 L/h.m^2). For BW30, the ratio increased from 0.22±0.08 for a flux of 0.5 L/h.m^2 to 0.27±0.11 for 13.7 L/h.m^2 up to 0.34±0.01 for 21.2 L/h.m^2. In the case of BW30 FR, the ratio did not substantially change throughout the studied permeate flux range, varying from 0.41±0.13 for a flux of 0.5 L/h.m^2 down to 0.33±0.02 for 21.2 L/h.m^2. For NF90, the ratio increased from 0.32±0.12 for a flux of 2.2 L/h.m^2 to 0.35±0.27 for 30.7 L/h.m^2 up to 0.41±0.03 for 40.0 L/h.m^2. Adhesion on ESNA1-LF led to a ratio

increase from 0.04±0.04 for a flux of 1.1 L/h.m^2 to 0.23±0.17 for 18.8 L/h.m^2 up to 0.25±0.04 for 28.8 L/h.m^2 , whilst adhesion on ESNA1-LF2 led to a ratio increase from 0.12±0.12 for a flux of 3.4 L/h.m^2 up to 0.27±0.16 for 45.5 L/h.m^2. In contrast membranes with high permeate fluxes showed the most significant increase in damaged cell ratio: the NF270 membrane had a ratio increase from 0.06±0.02 at 19 L/h.m^2 to 31±0.09 for 97.0 L/h.m^2 up to 0.83±0.04 for 116 L/h.m^2.

These results therefore indicate a positive correlation between damaged/live ratio of adhered cells with permeate flux, which is more pronounced for nanofiltration membranes with a wide range of permeate fluxes compared to tight nanofiltration/reverse osmosis membranes. A more in depth analysis is therefore needed to identify the specific mechanisms responsible for cell damage under permeate flux conditions.

Effect of hydrodynamic shear, permeate flux and filtration time on the structural integrity of Pseudomonas fluorescens cells during Nanofiltration.

The effect of different pressure-controlled permeate flux conditions and filtration configuration on the structural integrity of deposited *P. fluorescens* cells were investigated for the NF 270 and NF 90 membranes in cross-flow and dead-end mode operation for 30 minutes (Figure 2). The effect of filtration time was also assessed by performing dead-end NF experiments for 10 minutes (Figure 2).

The ratio of damaged cells versus total live cells on membranes following cross-flow filtration was found to be between 1.8 to 3 times higher than that following dead-end filtration for the same filtration conditions, regardless of the pressure conditions tested and membrane used. Although measured permeate fluxes were lower under cross-flow compared to dead-end filtration conditions (Table 2), the additional filtration configuration in the form of cross-flow velocity resulted in higher ratios of damaged cells through shear stress. Cell damage of adhered cells during NF processes is

therefore not solely caused by permeate flux conditions, but rather in combination with additional stress factors such as shear, which may lead to aggravated cell structural damage.

Table 2: Mean permeate fluxes during cell adhesion assays on either NF 270 or NF 90 membranes at different pressure conditions (3 bar or 15 bar) and filtration systems. Error represents standard error of the mean.

	Permeate Flux (L / h . m^2)			
	NF 270		NF 90	
	3 bar	15 bar	3 bar	15 bar
MET (Dead-end)	37.67 ± 0.60	174.46 ± 4.7	8.23 ± 0.30	58.03 ± 2.4
MFS (Cross-flow)	17.60 ± 0.04	115.66 ± 2.4	2.20 ± 0.04	40.04 ± 1.0

The NF270 membrane at 15 bar, which had the highest permeate fluxes of 174.4 L/h. m^2 for dead-end and 115.6 L/h. m^2 for cross-flow, lead to higher ratios of damaged cells of 41 % and 82%, respectively, whereas the NF 90 membrane under identical pressure conditions led to both lower permeate fluxes of 58 and 40 L/h. m^2, as well as lower ratios of damaged cells of 22% and 43%, under dead-end and cross-flow filtration conditions, respectively. At 3 bar pressure conditions, the permeate fluxes for the NF 270 membrane were of 37.6 L/h. m^2 for dead end and 17.6 L/h. m^2 for cross-flow and lead to the lowest observed ratios of damaged/live cell of 14% and 6%. These observations confirm that the degree of cell damage on membranes during NF processes is correlated to permeate flux. Interestingly, despite the lowest permeate flux conditions on NF 90 membranes at 3 bar pressure, the ratio of damaged cells were found to be similar to those on the NF 270 membrane for the same pressure under dead-end filtration conditions. This confirms that there is a minimum permeate flux by which the ratio of damaged cells starts increasing substantially, as suggested from Figure 1. In dead-end mode conditions, the ratio of damaged cells was found to be

around 15% at permeate fluxes lower than 40 L/h. m^2 and increased to 22% and 41% at higher permeate flux values of 58 and 174.4 L/h. m^2, respectively. The same occurred in cross-flow filtration conditions; the ratio of damaged cells was lower than 40% at permeate fluxes lower than 40 L/h. m^2, only to increase to 82% when higher permeate flux conditions were of 115.6 L/h. m^2.

These results suggest that the effect of permeate flux contributed significantly to structural damage of the adhered *P. fluorescens* cells, especially for fluxes above 58 L/h.m^2. Furthermore, increasing permeate flux during NF lead to higher damaged cell ratios, regardless of the tested membrane used. The additional cross-flow shear exacerbated cell stress and damage, by eroding the cell wall. This type of cell damage is comparable to that incurred following high speed centrifugation. A study by Gilbert et al (1991) demonstrated that Gram-negative cell wall material could be stripped off following centrifugation forces of 10 000 g in which hydrostatic pressures within a 15 mL centrifuge could attain 10 bar [31]. Furthermore, the bacterial cell surface is fragile and can be easily modified and damaged depending on the exerted force, as previously demonstrated by Grandbois et al (1999), where it was shown that most organic compounds constituting cell surface molecules anchored on the cell membrane are damaged at only 4.5 nN [32].

Another possible factor that might affect cell structural stability during adhesion in NF processes is the occurrence of concentration polarisation. Under permeate flux conditions, concentration polarisation is a phenomenon whereby concentration gradients of solutes present in the feed solution form at the membrane-liquid interface. In the present study it can be expected that as a result of concentration polarisation, the adhered bacterial cells are exposed to an elevated concentration of dissolved salt, and hence ionic strength. Bacterial cells are known to respond to osmolarity changes within their environment by adjusting their Turgor pressure through a strategic exoosmotic release of water [33], resulting in cell-shrinkage, the level of which would depend on solute concentration in the surrounding environment.

296 The calculated polarisation modulus for several experiments in dead-end and cross-flow
297 configuration are presented in Table 3 for 30 minutes of adhesion.

298

299 **Table 3** – Polarisation modulus at the end of 30 minutes for the NF90 and NF270 membranes in
300 dead-end and cross-flow mode

	Dead-end		Cross-flow	
	3 bar	15 bar	3 bar	15 bar
NF270	1.14 ± 0.06	2.68 ± 2.39	1.03 ± 0.003	1.46 ± 0.11
NF90	1.05 ± 0.01	1.66 ± 0.39	1.01 ± 0.002	1.47 ± 0.10

301

302 As can be seen in Table 3, in cross-flow mode both membranes had similar polarisation modulus
303 when subjected to the same hydrostatic pressure. The higher flux of the NF 270 membrane
304 compared to the NF 90 membrane balanced the lower retention of the NF 270 in regards to NaCl
305 retention compared to the NF 90 (see equation (1)). If concentration polarisation was in fact the
306 culprit for the higher ratio of damaged cells, then one would expect the same ratio for the NF 270
307 and the NF 90 membranes at 3 bar and the same ratio at 15 bar, since the polarisation modulus is
308 similar. However from Figure 2, the NF 270 has a higher ratio of damaged cells compared to the NF
309 90 membrane at 15 bar. This is linked to the fact that the NF 270 membrane has a higher permeate
310 flux compared to the NF 90 membrane (Table 2), allowing concluding that convection towards the
311 membrane surface causes cell damage. Furthermore, in dead-end experiments the permeate flux of
312 the NF 270 membrane at 3 bar was slightly lower than the one of the NF 90 at 15 bar (Table 2). The
313 polarisation modulus for the NF90 membrane however was 1.6 compared to 1.1 for the NF 270
314 membrane (Table 3). Despite their differences in polarisation modulus under similar permeate flux
315 conditions, the ratio of damaged cells on both NF 90 and NF 270 were relatively low at 25% and 15%,
316 respectively, with differences associated with variations in permeate fluxes. These results suggest
317 that concentration polarisation did not play a significant role in influencing the structural stability of

318 cells. This was further verified, by monitoring the electrophoretic mobility of *P. fluorescens* cells to
319 high salt concentrations (Cf. Supplementary Information; S3). Results showed that no significant
320 change in bacterial cell wall electronegativity occurred, even when exposed to extreme high salt
321 concentrations. Nevertheless, changes in cell membrane physicochemical and dynamic properties
322 may occur as a direct consequence of increased solute concentration. In one recent study
323 investigating the effects of bulk medium ionic strengths on the morphological, nanomechanical and
324 electrohydrodynamic properties of different *Escherichia coli* K-12 cell wall mutants, Francius et al
325 (2011) showed that bacterial exoosmotic water loss at high salt concentrations resulted in a
326 combined contraction of bacterial cytoplasm together with an electrostatically-driven shrinkage of
327 the surface appendages, which also led to a decrease in cell electronegativity [34]. This change in
328 physicochemical properties could favour bacterial adhesion, as well as cell to cell aggregation, as
329 explained by the DLVO, XDLVO theory [35, 36].

330 To determine whether the observed damaged cell ratios were time dependant, adhesion
331 experiments were also carried out for 10 minutes using a dead-end filtration system and compared
332 with ratios following 30 minute adhesion experiments (Figure 2). Interestingly higher damaged cell
333 ratios were observed at 30 minutes compared to 10 minutes deposition periods regardless of the
334 pressure: 4 and 2.8 times higher at 3 bar and 15 bar, respectively, for the NF 270 membrane, and 15
335 and 2.3 times higher at 3 bar and 15 bar, respectively, for the NF 90 membrane. Higher damaged to
336 live cell ratios in situations of lower permeate flux under cross-flow filtration further confirms that
337 active shear forces over the course of high pressure nanofiltration does cause damage to adhered
338 cells. Corresponding total number of adhered cells for each filtration experiments is provided in the
339 supplementary information section (Table S4). Increasing exposure time under the same permeate
340 flux conditions further increases the level of cell damage.

341 Dead-end filtration was chosen in combination with flow cytometry to qualitatively assess the
342 structural fate of deposited cells onto NF membranes as they are subjected to physical compaction

onto the membrane caused by the permeate flux, as well as exposed to different ionic concentrations caused by concentration polarisation (Figure 3 & 4). The NF 270 membrane was selected given its higher permeate flux properties at 15 bar pressure conditions compared to NF 90 membranes. To ensure sufficient retentate sampling following dead-end filtration, the filtration experiment was stopped after 15 minutes.

Prior to filtration (control), the suspension of *Pseudomonas fluorescens* cells was composed of 3.27% ± 1.33% damaged cells (Q1) , 4.69% ± 4.7 % partially damaged cells (Q2), 71.55% ± 4.73% healthy cells (Q3) and 16.9% ± 5.23% debris (Q4) (Figure 3). No significant differences were observed for non-deposited cells in the bulk liquid after dead-end filtration compared to cells prior filtration (p=1.00). The bulk suspension population was composed of 3.0% ± 0.46% (Q1); 5.0% ± 4.58% (Q2), 69.0% ± 3.6% (Q3,) and 17.0% ± 0.91% (Q4) (Figure 3). This shows that pressure alone did not impact on the structural integrity of the cells, as the cells in the bulk liquid subjected to 15 bar show no statistical difference from the ones in the control.

Changes in population fractions were observed for deposited cells on the membranes compared to cells prior to filtration (Figure 3). The damaged cell fraction (Q1) was composed of 11.27 % ± 6.97%, while the partially damaged fraction was composed of 17.09 % ± 12.1%. The fraction of healthy cells significantly reduced to 38.3% ± 15.83% compared to the healthy cell fraction prior to filtration (p= 0.013). Moreover the fraction of debris also increased to 29.6 % ± 3.95 %. These results not only confirmed epi-fluorescence microscopy observations previously shown, but also expose the resulting increased level of debris fraction following NF, a tell-tale sign of eroded bacterial cell wall components, disintegrated cells and even relinquished cytoplasmic material. The consequential abrasion of cell membrane molecules resulting from exposure to high shear forces in cross-flow during NF could have led to imbalances of cell wall components resulting in the weakening of the bacterial skeletal structure, potentially resulting in cell collapse. The highly elastic properties of the

368 bacterial cell wall, known to withstand pressures up to 1000 bar, has been thoroughly described in
369 the literature [37, 38]. Moreover several studies have shown that while maintaining a relatively
370 compliant cell elasticity under normal condition, bacterial cell wall stiffens as a direct response to
371 tensile stress, hence providing the cells with a unique mechanical advantage by preventing abrupt
372 changes in cell morphology [39]. However, the combined effect of hydrodynamic shear, collision shear
373 and convective flux encountered at the membrane surface during nanofiltration may lead to shear
374 injuries localised on bacterial cell wall during deposition. Fluid mechanical stress caused by
375 hydrodynamic shear have been shown to induce cell damage and cell death in mammalian cells [40, 41]
376 as well as in bacterial cell [42], causing cell collapse and disintegration.
377 Further SEM analysis of sorted cells (Figure 4) revealed that sorted SYTOX Green positive cells prior
378 to filtration (Figure 4 A and corresponding SEM micrographs) were structurally more intact than
379 sorted cells following compaction on the membrane which showed signs of structural weakness. As
380 can be seen in Figure 4 C and the first corresponding SEM micrographs, the bacterial cell membrane
381 wall is compromised, with intracellular material being released in contrast with the bacteria showed
382 in the adjacent SEM micrographs which shows no cell wall integrity issues. Although one recent
383 study demonstrated that most cells suffer cataclysmic wall failure in situations where cell turgor is
384 increased [43], the results presented in this study indicate that compaction associated with shear
385 stress can potentially lead to cell collapse.
386

387 ***Hydrodynamic shear mediated cell death: a possible precursor to biofouling during nanofiltration.***
388 To further investigate the resulting effect of NF on bacterial cells, SEM of the membranes following
389 adhesion experiments were performed to qualitatively assess the different populations identified
390 from flow cytometry analysis (Figure 4). Filtration experiments on NF 270 membranes at 15 bar for
391 15 minutes revealed an abundance of both damaged/collapsed, and intact cells, as well as what
392 looked like cell debris, as shown on Figure 5. Some of the collapsed cells clearly demonstrated signs

of relinquishing intracellular material (Figure 5 A-B-C-D-F), which in some cases was also associated with cells that had clumped.

Based on these observations, the presence of cell debris originating from collapsed cells may potentially serve as a way to recruit planktonic cells, helping them to consolidate onto the membrane. One recent study showed that DNA released from cells during lysis, becomes a key component of the macromolecular scaffold in many different biofilms [44]. Although, cell death has been recognised as playing a significant role in biofilm formation [45], the phenomena at the membrane liquid interface described in this study may constitute another identified mechanism through which cytoplasmic cell material is released to the environment. Such a release may not only speed up the biofilm formation process, but may serve as a "nutrient rich cushion" on which new cells may thrive on and consolidate on the membrane. Additionally, the properties of the cytoplasmic material may also contribute in the recruitment of planktonic cells from the environment, enabling them to anchor down on the membrane surface and protect them from shear stress during nanofiltration. In one recent study, Petterson et al (2013) demonstrated the important role of extracellular DNA in biofilms was attributed to its viscoelastic relaxation properties providing embedded cells with protection against chemical and mechanical stresses [46].

The work described in this paper investigated the extent of damage of adhered bacterial cells during high pressure NF processes. Exposure times of up to 30 minutes at high permeate flux conditions at 15 bar was shown to have significantly damaged *P. fluorescens* cells, irrespective of cross-flow or dead-end filtration type systems. Cells adhering to membranes over the course of NF undergo substantial levels of stress affecting their structural integrity, ultimately leading to the release of cytoplasmic material onto the membrane. This could be an important element in biofilm formation by providing embedded cells protection against chemical and mechanical stresses. This study identifies cell lysis as a possible missing link in the membrane biofouling story, a relevant step

between initial cell adhesion and subsequent biofilm formation during nanofiltration. Further studies, however, need to be carried out in order to confirm whether cell damage caused by cross-flow and permeate flux indeed enhances biofilm formation. Such studies should include bacterial physiological response to permeate flux conditions. This can be achieved by exposing bacterial cells to metabolic inhibitors or bacteriostatic antibiotics prior to adhesion assays, to determine whether cell damage is induced by solely physical means or through an active response from individual cells.

Acknowledgments

This research was supported by the European Research Council (ERC), project 278530, funded under the EU Framework Programme 7. The authors would like to thank Mr. Liam Morris for the construction of the MFS devices and Mr Colm Lynch, from GKA Technologies (Ireland) for providing the MET dead-end cells; Dr. Alfonso Blanco-Fernandez and Dr. Ann Cullen of the Conway Institute Flow Cytometry Core facility for their assistance with flow cytometry experiments and analysis; and Dr. Ian Reid of the NIMAC microscopy platform UCD and Ms. Ashley Allen for their assistance with scanning electron microscopy. The authors especially thank Dr. Ellen L. Lagendijk from the Institute of Biology Leiden, Netherlands, for the gift of the mCherry-tagged *Pseudomonas fluorescens* PCL 1701 strain. Professor Geoffrey Hamer is acknowledged for critical reading and comments of this manuscript. Hydranautics is also thanked for the supply of the ESNA1-LF and ESNA1-LF2 membranes.

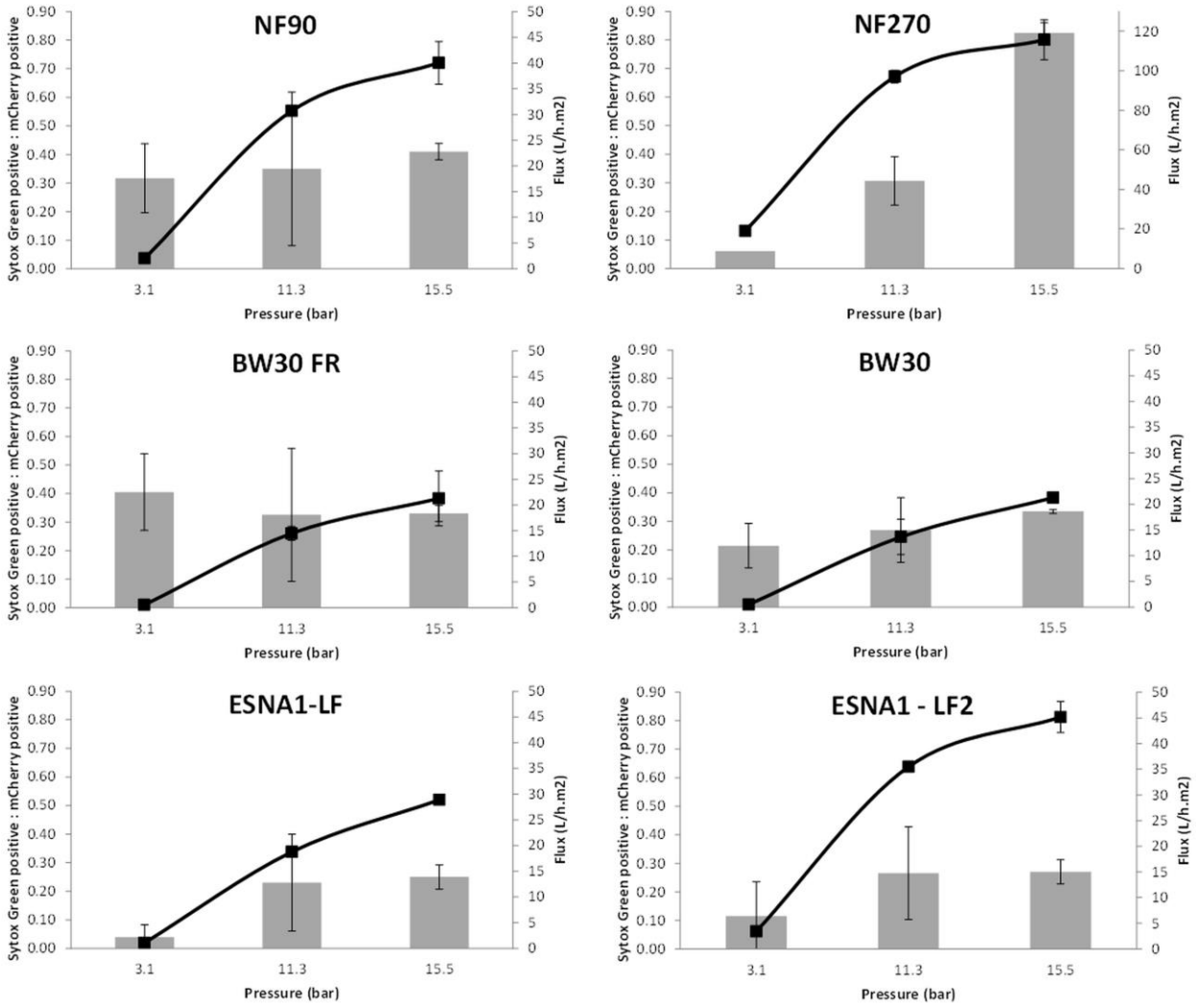

Figure 1 - Ratio of damaged cells to live cells of adhered *Pseudomonas fluorescens* cells onto six NF/RO membranes in a cross-flow system (columns) as a function of permeate flux (black squares): NF 270, NF 90, BW30 FR, BW30, ESNA1-LF, ESNA1-LF2 (10^7 cells/mL of *P. fluorescens* in 0.1 M NaCl, 30 minute adhesion, cross-flow conditions: 21°C, pH~7, 0.66 $L.min^{-1}$ or Re=579 in each MFS cell). Adhesion assays were performed in at least two independent experiments. Error bars represent standard error of the mean. (Note: the permeate flux is apparently not seen as a linear relationship with pressure because the columns are not equally spaced in pressure. The linear correlation coefficient of permeate flux vs pressure is in fact $r^2>0.995$ for these experiments)

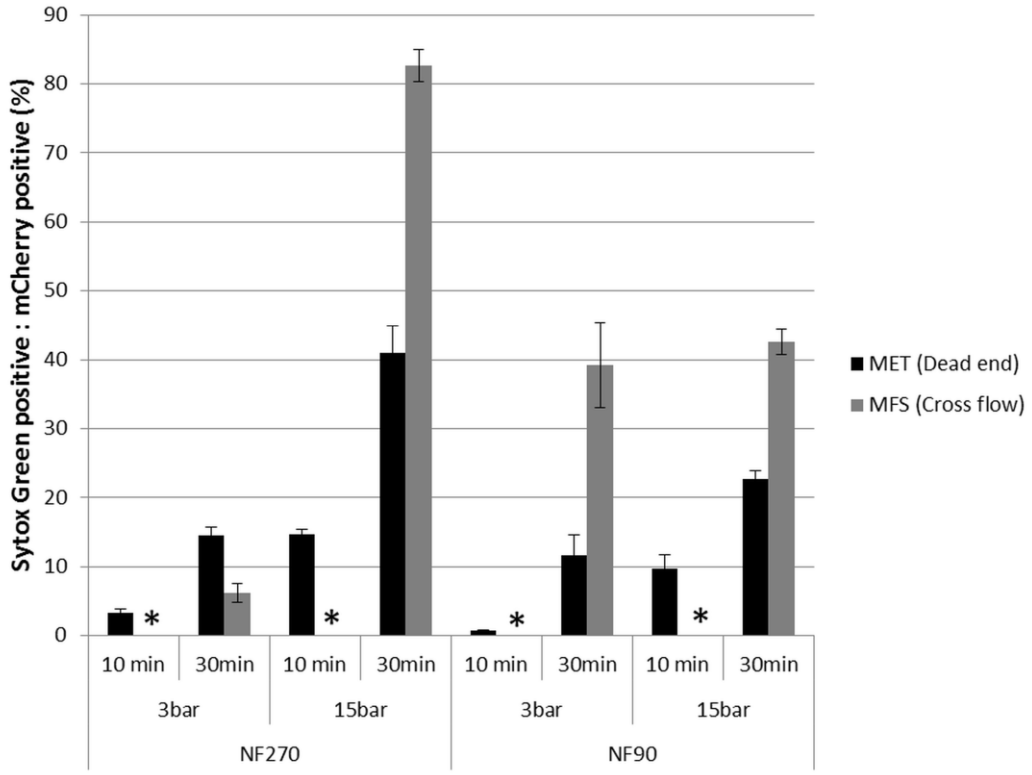

455 * Not Determined

456 **Figure 2:** The ratio of damaged cells to live cells based on acquired SYTOX Green and mCherry
457 positive signals of adhered *Pseudomonas fluorescens* cells on NF 270 and NF 90 membranes,
458 following nanofiltration using either cross-flow or dead-end type systems. Adhesion assays were
459 performed in at least three independent experiments. Error bars represent standard error of the
460 mean.

461

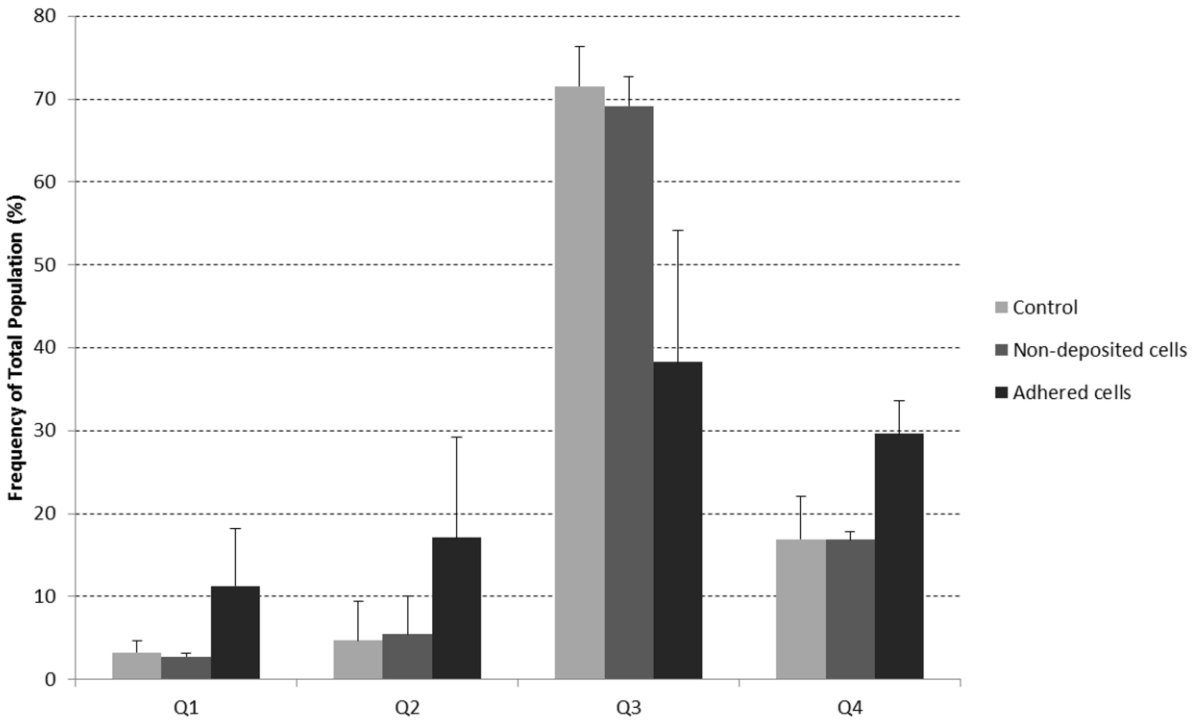

462

463 **Figure 3:** Mean population fractions of *Pseudomonas fluorescens* cells prior to dead-end filtration
464 (control), and after dead-end filtration from the remaining bulk retentate volume (Non-deposited
465 cells) and the membrane (Adhered cells). The dead-end filtration conditions were 15 bar, 15
466 minutes, NF270 membrane and 150 rpm. Population frequencies (%) were divided into 4 quadrants
467 (Q1-Q4) obtained following FACS data analysis based on mCherry and SYTOX Green fluorescence
468 intensities (Cf. Supplementary information; S2). Q1 represent the fraction of mCherry negative and
469 SYTOX Green positive cells (Damaged cells), Q2 equates to mCherry positive and SYTOX Green
470 positive cells (partially damaged cells), Q3 is associated with mCherry positive and SYTOX Green
471 negative cells (healthy cells), while Q4 clusters mCherry negative and SYTOX Green negative cells
472 (Debris). FACS was performed in at least two independent experiments. Error bars represent
473 standard deviation of the mean.

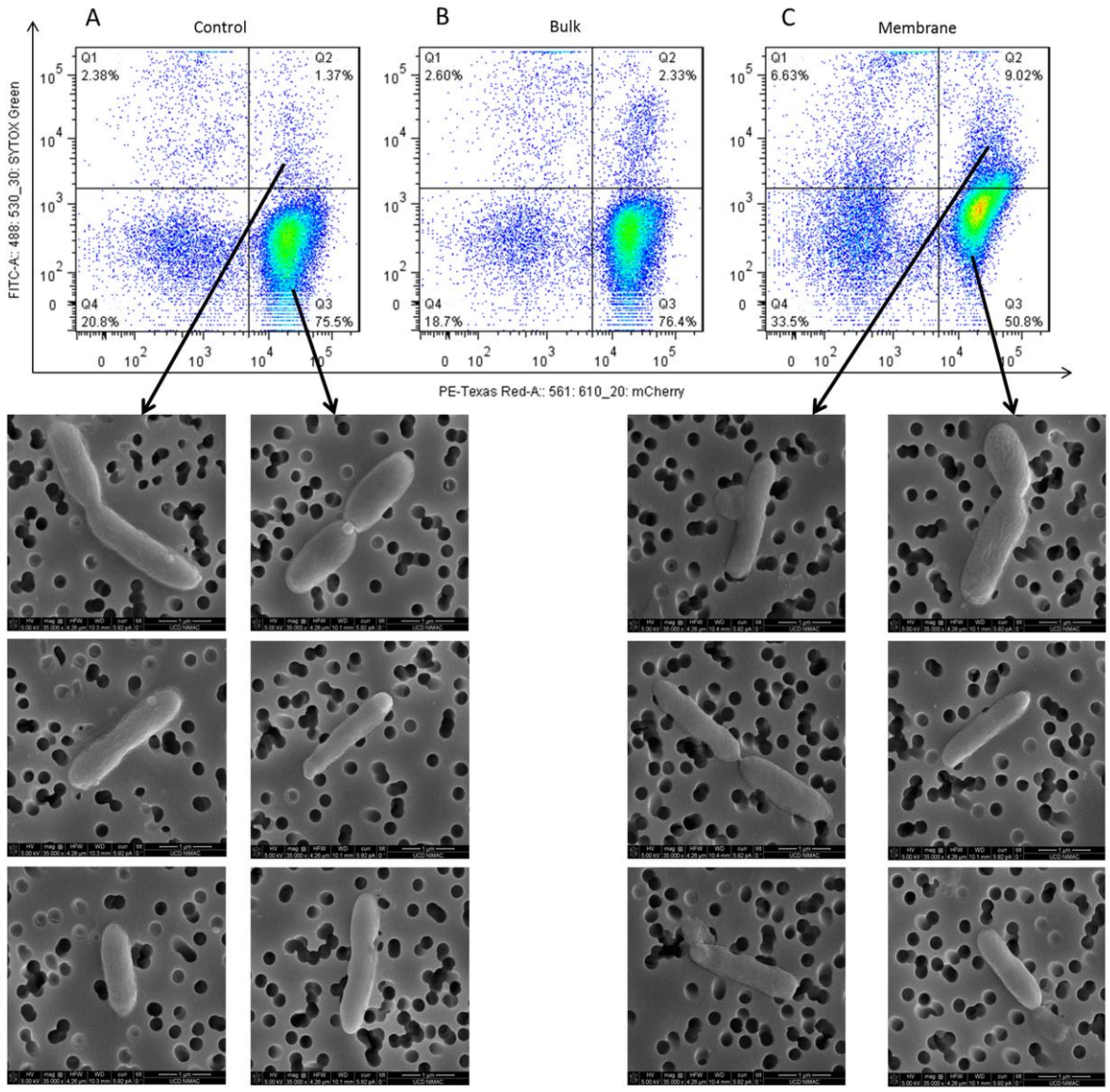

474

475 **Figure 4**: Population shifts from healthy cells (mCherry positive) to damaged cells (SYTOX Green
476 positive) following deposition at 15 bar pressure conditions on NF 270 membrane. Representative
477 plots from three separate filtration experiments show the gated suspended *Pseudomonas*
478 *fluorescens* cells (A) prior to dead-end filtration, (B) non-deposited cells in the retentate following
479 dead-end filtration and (C) re-suspended deposited cells following dead-end filtration. Scanning
480 electron micrographs of sorted cells from selected gated populations was performed for comparing
481 cells prior and after dead-end filtration at 15 bar.

482

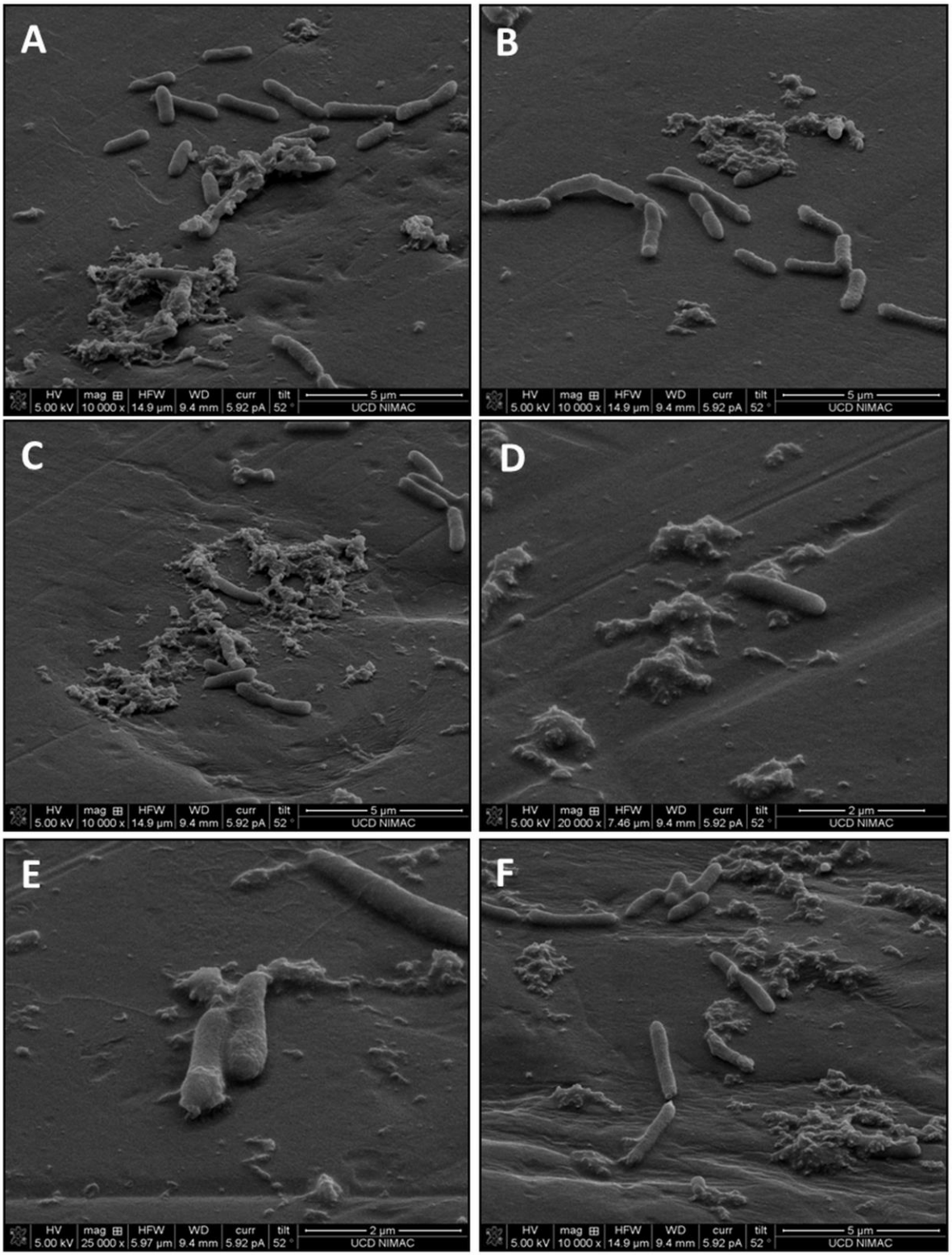

Figure 5: Scanning electron micrographs of fouled NF 270 membranes following dead-end nanofiltration for 15 minutes at 15 bar. Representative micrographs (ABCDEF) were obtained depicting the fate of *P. fluorescens* cell on following dead-end nanofiltration for 15 minutes at 15 bar.

References

1. Cyna, B.; Chagneau, G.; Bablon, G.; Tanghe, N., Two years of nanofiltration at the Méry-sur-Oise plant, France. *Desalination* **2002,** *147*, (1–3), 69-75.
2. Flemming, H. C., Reverse osmosis membrane biofouling. *Exp Therm Fluid Sci* **1997,** *14*, (4), 382-391.
3. Ivnitsky, H.; Katz, I.; Minz, D.; Volvovic, G.; Shimoni, E.; Kesselman, E.; Semiat, R.; Dosoretz, C. G., Bacterial community composition and structure of biofilms developing on nanofiltration membranes applied to wastewater treatment. *Water Res* **2007,** *41*, (17), 3924-3935.
4. Flemming, H. C., Biofouling in water systems – cases, causes and countermeasures. *Applied Microbiology and Biotechnology* **2002,** *59*, (6), 629-640.
5. Houari, A.; Seyer, D.; Couquard, F.; Kecili, K.; Démocrate, C.; Heim, V.; Martino, P. D., Characterization of the biofouling and cleaning efficiency of nanofiltration membranes. *Biofouling* **2009,** *26*, (1), 15-21.
6. Vrouwenvelder, H. S.; van Paassen, J. A. M.; Folmer, H. C.; Hofman, J. A. M. H.; Nederlof, M. M.; van der Kooij, D., Biofouling of membranes for drinking water production. *Desalination* **1998,** *118*, (1–3), 157-166.
7. Vrouwenvelder, J. S.; Manolarakis, S. A.; van der Hoek, J. P.; van Paassen, J. A. M.; van der Meer, W. G. J.; van Agtmaal, J. M. C.; Prummel, H. D. M.; Kruithof, J. C.; van Loosdrecht, M. C. M., Quantitative biofouling diagnosis in full scale nanofiltration and reverse osmosis installations. *Water Res* **2008,** *42*, (19), 4856-4868.
8. Khan, M. T.; Manes, C.-L. d. O.; Aubry, C.; Croué, J.-P., Source water quality shaping different fouling scenarios in a full-scale desalination plant at the Red Sea. *Water Res* **2013,** *47*, (2), 558-568.
9. Hijnen, W. A. M.; Castillo, C.; Brouwer-Hanzens, A. H.; Harmsen, D. J. H.; Cornelissen, E. R.; van der Kooij, D., Quantitative assessment of the efficacy of spiral-wound membrane cleaning procedures to remove biofilms. *Water Res* **2012,** *46*, (19), 6369-6381.
10. Ivnitsky, H.; Katz, I.; Minz, D.; Shimoni, E.; Chen, Y.; Tarchitzky, J.; Semiat, R.; Dosoretz, C. G., Characterization of membrane biofouling in nanofiltration processes of wastewater treatment. *Desalination* **2005,** *185*, (1–3), 255-268.
11. Huertas, E.; Herzberg, M.; Oron, G.; Elimelech, M., Influence of biofouling on boron removal by nanofiltration and reverse osmosis membranes. *J Membrane Sci* **2008,** *318*, (1–2), 264-270.
12. Habimana, O.; Semiao, A. J. C.; Casey, E., The role of cell-surface interactions in bacterial initial adhesion and consequent biofilm formation on nanofiltrationfreverse osmosis membranes. *J Membrane Sci* **2014,** *454*, 82-96.
13. Ridgway, H. F.; Rigby, M. G.; Argo, D. G., Bacterial Adhesion and Fouling of Reverse Osmosis Membranes. *Journal of American Water Works Association* **1985,** *77*, (7), 97-106.
14. Subramani, A.; Hoek, E. M. V., Direct observation of initial microbial deposition onto reverse osmosis and nanofiltration membranes. *J Membrane Sci* **2008,** *319*, (1–2), 111-125.
15. Myint, A. A.; Lee, W.; Mun, S.; Ahn, C. H.; Lee, S.; Yoon, J., Influence of membrane surface properties on the behavior of initial bacterial adhesion and biofilm development onto nanofiltration membranes. *Biofouling* **2010,** *26*, (3), 313-321.
16. Khan, M. M. T.; Stewart, P. S.; Moll, D. J.; Mickols, W. E.; Nelson, S. E.; Camper, A. K., Characterization and effect of biofouling on polyamide reverse osmosis and nanofiltration membrane surfaces. *Biofouling* **2011,** *27*, (2), 173-183.
17. Subramani, A.; Huang, X.; Hoek, E. M. V., Direct observation of bacterial deposition onto clean and organic-fouled polyamide membranes. *J Colloid Interf Sci* **2009,** *336*, (1), 13-20.

18. Costerton, J. W.; Lewandowski, Z.; Caldwell, D. E.; Korber, D. R.; Lappin-Scott, H. M., Microbial biofilms. *Annual Reviews in Microbiology* **1995,** *49*, (1), 711-745.
19. Lee, W.; Ahn, C. H.; Hong, S.; Kim, S.; Lee, S.; Baek, Y.; Yoon, J., Evaluation of surface properties of reverse osmosis membranes on the initial biofouling stages under no filtration condition. *J Membrane Sci* **2010,** *351*, (1–2), 112-122.
20. Bernstein, R.; Belfer, S.; Freger, V., Bacterial Attachment to RO Membranes Surface-Modified by Concentration-Polarization-Enhanced Graft Polymerization. *Environ Sci Technol* **2011,** *45*, (14), 5973-5980.
21. Sadr Ghayeni, S. B.; Beatson, P. J.; Schneider, R. P.; Fane, A. G., Adhesion of waste water bacteria to reverse osmosis membranes. *J Membrane Sci* **1998,** *138*, (1), 29-42.
22. Herzberg, M.; Elimelech, M., Biofouling of reverse osmosis membranes: Role of biofilm-enhanced osmotic pressure. *J Membrane Sci* **2007,** *295*, (1–2), 11-20.
23. Chong, T. H.; Wong, F. S.; Fane, A. G., The effect of imposed flux on biofouling in reverse osmosis: Role of concentration polarisation and biofilm enhanced osmotic pressure phenomena. *J Membrane Sci* **2008,** *325*, (2), 840-850.
24. Baek, Y.; Yu, J.; Kim, S.-H.; Lee, S.; Yoon, J., Effect of surface properties of reverse osmosis membranes on biofouling occurrence under filtration conditions. *J Membrane Sci* **2011,** *382*, (1–2), 91-99.
25. Speth, T. F.; Summers, R. S.; Gusses, A. M., Nanofiltration Foulants from a Treated Surface Water. *Environ Sci Technol* **1998,** *32*, (22), 3612-3617.
26. Lagendijk, E. L.; Validov, S.; Lamers, G. E.; de Weert, S.; Bloemberg, G. V., Genetic tools for tagging Gram-negative bacteria with mCherry for visualization in vitro and in natural habitats, biofilm and pathogenicity studies. *FEMS Microbiol Lett* **2010,** *305*, (1), 81-90.
27. King, E. O.; Ward, M. K.; Raney, D. E., Two simple media for the demonstration of pyocyanin and fluorescin. *J Lab Clin Med* **1954,** *44*, (2), 301-7.
28. Semião, A. J. C.; Habimana, O.; Cao, H.; Heffernan, R.; Safari, A.; Casey, E., The importance of laboratory water quality for studying initial bacterial adhesion during NF filtration processes. *Water Res* **2013,** *47*, (8), 2909-2920.
29. Semião, A. J. C.; Schäfer, A. I., Estrogenic micropollutant adsorption dynamics onto nanofiltration membranes. *J Membrane Sci* **2011,** *381*, (1–2), 132-141.
30. Bowen, W. R.; Mohammad, A. W.; Hilal, N., Characterisation of nanofiltration membranes for predictive purposes - use of salts, uncharged solutes and atomic force microscopy. *J Membrane Sci* **1997,** *126*, (1), 91-105.
31. Gilbert, P.; Caplan, F.; Brown, M. R. W., Centrifugation Injury of Gram-Negative Bacteria. *Journal of Antimicrobial Chemotherapy* **1991,** *27*, (4), 550-551.
32. Grandbois, M.; Beyer, M.; Rief, M.; Clausen-Schaumann, H.; Gaub, H. E., How strong is a covalent bond? *Science* **1999,** *283*, (5408), 1727-1730.
33. Marquis, R. E., Salt-Induced Contraction of Bacterial Cell Walls. *Journal of Bacteriology* **1968,** *95*, (3), 775-781.
34. Francius, G.; Polyakov, P.; Merlin, J.; Abe, Y.; Ghigo, J. M.; Merlin, C.; Beloin, C.; Duval, J. F. L., Bacterial Surface Appendages Strongly Impact Nanomechanical and Electrokinetic Properties of Escherichia coli Cells Subjected to Osmotic Stress. *Plos One* **2011,** *6*, (5).
35. Derjaguin, B.; Landau, L., Theory of Stability of Highly Charged Liophobic Sols and Adhesion of Highly Charged Particles in Solutions of Electrolytes. *Zhurnal Eksperimentalnoi I Teoreticheskoi Fiziki* **1945,** *15*, (11), 663-682.
36. Vanoss, C. J.; Chaudhury, M. K.; Good, R. J., Interfacial Lifshitz-Vanderwaals and Polar Interactions in Macroscopic Systems. *Chemical Reviews* **1988,** *88*, (6), 927-941.
37. Follonier, S.; Panke, S.; Zinn, M., Pressure to kill or pressure to boost: a review on the various effects and applications of hydrostatic pressure in bacterial biotechnology. *Applied Microbiology and Biotechnology* **2012,** *93*, (5), 1805-1815.

587 38. Hartmann, C.; Mathmann, K.; Delgado, A., Mechanical stresses in cellular structures under
588 high hydrostatic pressure. *Innovative Food Science & Emerging Technologies* **2006,** *7*, (1-2), 1-12.
589 39. Deng, Y.; Sun, M. Z.; Shaevitz, J. W., Direct Measurement of Cell Wall Stress Stiffening and
590 Turgor Pressure in Live Bacterial Cells. *Physical Review Letters* **2011,** *107*, (15).
591 40. Rahimzadeh, J.; Meng, F. J.; Sachs, F.; Wang, J. B.; Verma, D.; Hua, S. Z., Real-time
592 observation of flow-induced cytoskeletal stress in living cells. *American Journal of Physiology-Cell*
593 *Physiology* **2011,** *301*, (3), C646-C652.
594 41. Brindley, D.; Moorthy, K.; Lee, J. H.; Mason, C.; Kim, H. W.; Wall, I., Bioprocess forces and
595 their impact on cell behavior: implications for bone regeneration therapy. *J Tissue Eng* **2011,** *2011*,
596 620247.
597 42. Thomas, R. J.; Webber, D.; Hopkins, R.; Frost, A.; Laws, T.; Jayasekera, P. N.; Atkins, T., The
598 cell membrane as a major site of damage during aerosolization of Escherichia coli. *Appl Environ*
599 *Microbiol* **2011,** *77*, (3), 920-5.
600 43. Reuter, M.; Hayward, N. J.; Black, S. S.; Miller, S.; Dryden, D. T.; Booth, I. R.,
601 Mechanosensitive channels and bacterial cell wall integrity: does life end with a bang or a whimper?
602 *J R Soc Interface* **2014,** *11*, (91), 20130850.
603 44. Jakubovics, N. S.; Shields, R. C.; Rajarajan, N.; Burgess, J. G., Life after death: the critical role
604 of extracellular DNA in microbial biofilms. *Letters in applied microbiology* **2013,** *57*, (6), 467-75.
605 45. Bayles, K. W., The biological role of death and lysis in biofilm development. *Nature Reviews*
606 *Microbiology* **2007,** *5*, (9), 721-726.
607 46. Peterson, B. W.; van der Mei, H. C.; Sjollema, J.; Busscher, H. J.; Sharma, P. K., A
608 distinguishable role of eDNA in the viscoelastic relaxation of biofilms. *Mbio* **2013,** *4*, (5), e00497-13.
609
610

611

Supporting Information:

Upon impact: the fate of adhering *Pseudomonas fluorescens* cells during Nanofiltration

Olivier Habimana[1], Andrea J.C. Semião[2], Eoin Casey[1]*

Supporting Information: S1

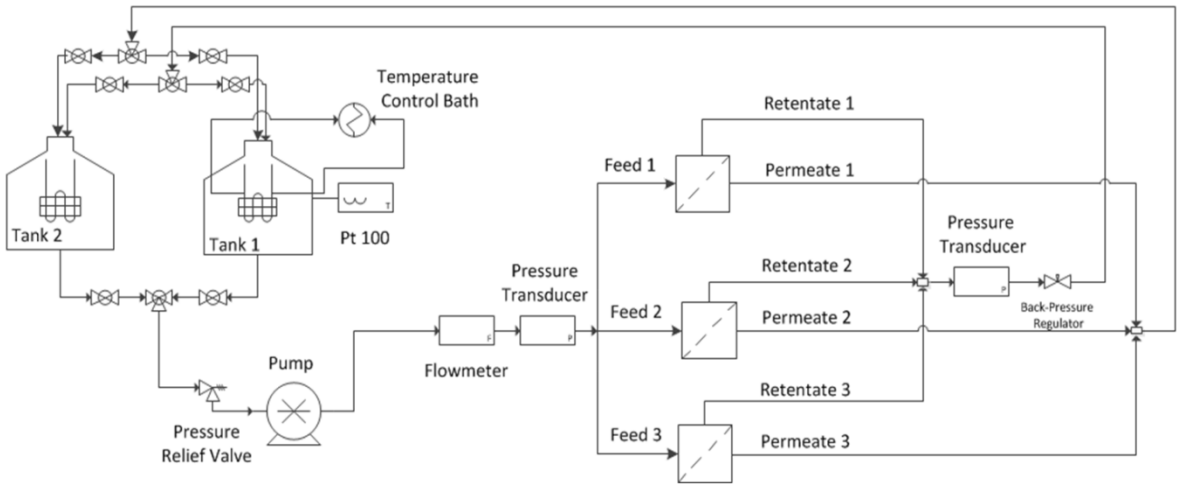

Figure S1. Cross-flow system used for the bacterial adhesion experiments under permeate flux conditions

The experimental system was designed as a loop arrangement comprising; two parallel autoclavable 10L feed tanks (Nalgene, VWR Ireland), a high pressure pump (P200 Hydra Cell, UK) and an array of three Membrane Fouling Simulator (MFS) devices (Internal channel dimensions: 0.8mm in height, 40 mm width and 255 mm length) positioned in parallel. Each MFS holds a membrane of approximately 102 cm^2. The loop arrangement allowed the recirculation of both retentate and permeates of each MFS. The P&ID of the crossflow filtration system is depicted in Figure S1.

A ball valve system at the inlet and outlet of each tank allowed the interchanging of flow between tanks during filtration and rinsing operations. Temperature was monitored during

630 filtration in one of the feed tanks with a temperature probe (Pt 100, Radionics, Ireland) and
631 maintained at 20ºC ± 1ºC with a heating/cooling coil inside the tank, which was connected
632 to a temperature controlled MultiTemp III water bath (Pharmacia Biotech, Ireland). A back
633 pressure regulator (KPB1L0A415P20000, Swagelok, UK) allowed the pressurization of the
634 system. The pressure was monitored in both feed and retentate side of the membrane cells
635 with two pressure transducers (PTX 7500, Druck, Radionics, Ireland). The feed flow was
636 measured using a flow meter (OG2, Nixon Flowmeters, UK). Datalogging was set-up allowing
637 the collection data from membrane cells inlet and outlet pressures, feed flow rate and
638 temperature (PicoLog 1000, PicoTechnology, Radionics, Ireland). The permeate flux was
639 determined by measuring a volume of permeate with a balance HCB123 balance (Adams,
640 Astech Ireland) at different time intervals using a stopwatch.
641
642
643
644
645
646
647
648
649
650
651
652
653
654
655
656
657
658
659

660 Supporting Information: S2

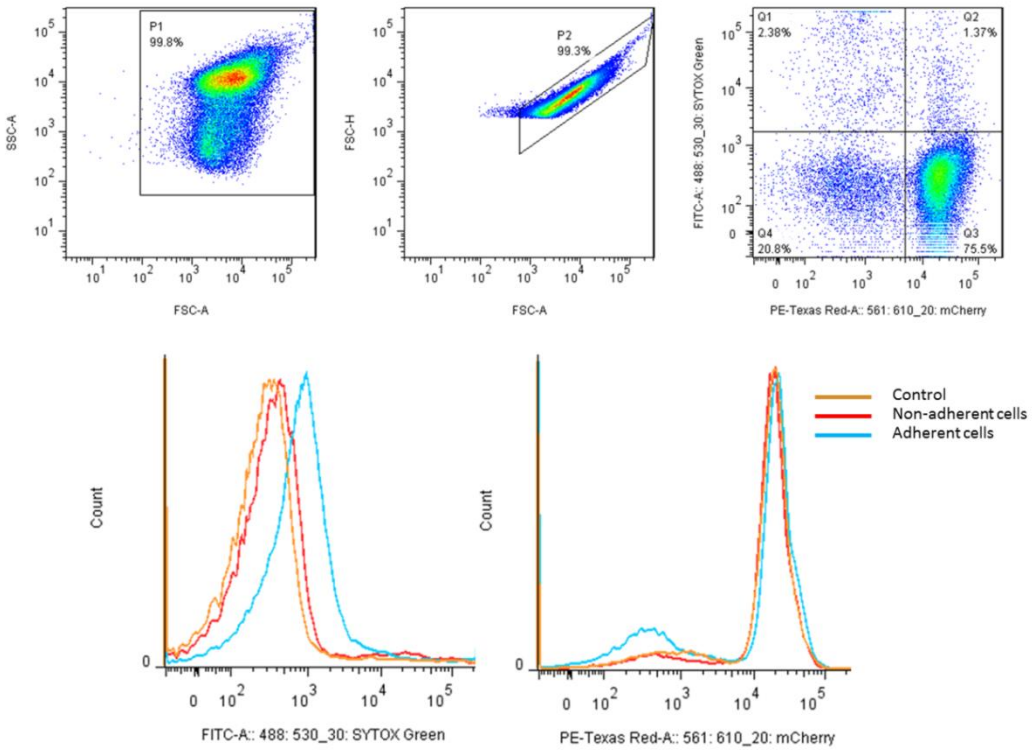

661

662 **Figure S2. Gating strategy for the analysis of *Pseudomonas fluorescens* cell wall structural**
663 **integrity following dead –end nanofiltration at 15 bar for 15 minutes.**

664 mCherry-expressing *Pseudomonas fluorescens* PCL1701 cells were labelled with SYTOX
665 green. This allowed the gating of four subset populations based on their SYTOX green and
666 mCherry fluorescence intensities.

667 The top left dot plot depicts cells in a live gate based on forward scatter and side scatter;
668 top central plot depicts gated cells based on forward scatter-area and forward scatter-
669 height for the selection of a uniform homogenous population of single-cells; top right dot
670 plot represent gating based on SYTOX green and mCherry fluorescence intensities.

671 The following gating strategies were applied for all tested samples:

672 Q1 :mCherry negative and SYTOX green positive cells (damaged cells),

673 Q2 : mCherry positive and SYTOX green positive cells (partially damaged cells)

674 Q3:mCherry positive and SYTOX green negative cells (healthy cells)

675 Q4:mCherry negative and SYTOX green negative cells (debris).

676 The bottom histograms show the proliferation of *Pseudomonas fluorescens* labelled with
677 SYTOX green positive (bottom left) or based on their mCherry expression (bottom right)
678 before and after dead-end filtration. Note that adhered cells following dead-end filtration
679 present an increased SYTOX green intensity coupled with an increased fraction of mCherry
680 negative cells compared to control cells and non-deposited cells.

Supporting Information: S3

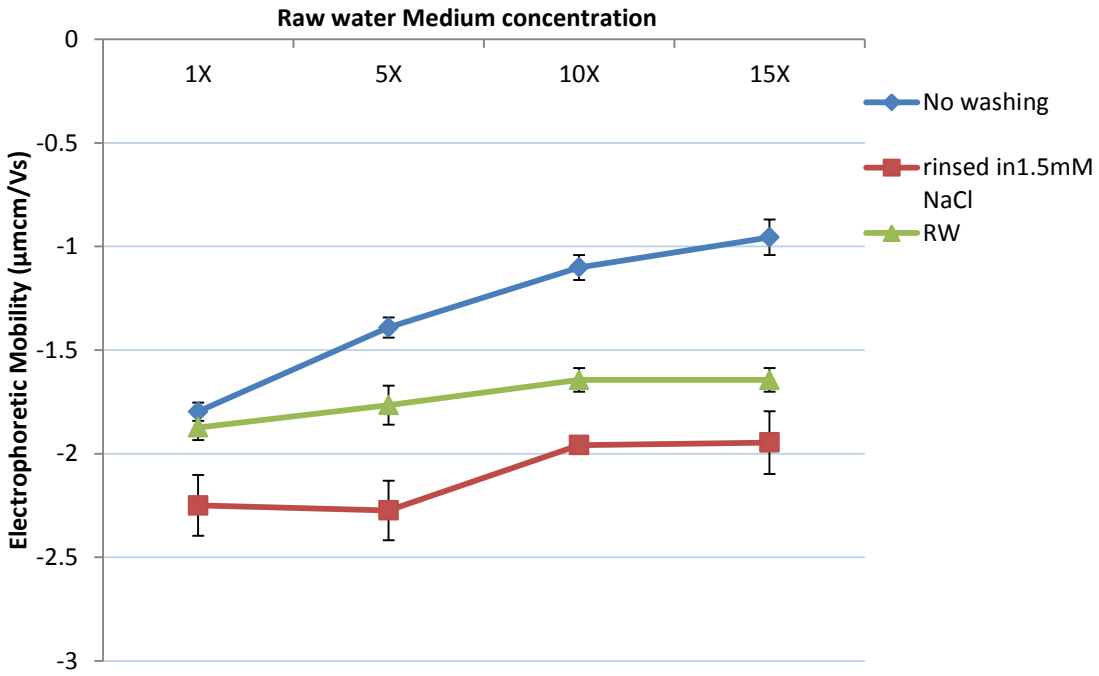

Figure S3. The effect of 15 minutes exposure of *Pseudomonas fluorescens* cells to increasing raw water salt concentrations in terms of changes in electrophoretic mobility.

To assess the potential role of exposure to high ionic strength environments on bacterial cell charge, experiments were performed in which centrifuged cell pellets were re-suspended in raw water medium solutions without carbon source (NaHCO3 0.042 g.L -1,NaCl 0.12 g.L -1,KH2PO4 0.063 g.L -1, MgSO4 0.15 g.L -1, NH4Cl 0.005 g.L -1, CaCl2 0.076 g.L -1) each having different salt concentrations levels of 5X, 10X and 15X, for an exposure period of 15 minutes. After exposure time, suspended cells were centrifuged (6000 RPM for 10min) and suspended to standard Raw water solution prior to electrophoretic mobility experiments using a zetasizer instrument (Malvern Zetasizer Nano ZS, Masontechnology, Dublin, Ireland).

Results presented in figure S3, show that washed cells, following 15 minutes exposure to high salt concentrations environments were not altered in terms of their surface charge as seen by the constant electrophoretic with increasing salt levels. Non-washed cells, still exposed to high salt concentrations, saw their surface charge become less electronegative with increasing salt concentrations. A constant electrophoretic mobility following high salt exposures is indicative of an undisturbed cell wall. When washed with in low ionic strength solution following salt exposures, the surface charge was noticeably altered following exposures to salt concentration 10x and 15x the normal RW- medium concentrations. This change in surface charge could have been direct results of osmotic stress which may have contributed to changes to cell wall as observed with a sudden lose in electronegativity.

Table S4: Estimated average Number of adhered *Pseudomonas fluorescens* cells /cm^2 membrane, based on surface coverage data following Nanofiltration using either cross-flow or dead-end type systems.

	NF270				NF90			
Nb cells/cm2	3bar		15bar		3bar		15bar	
	10 min	30min	10 min	30min	10 min	30min	10 min	30min
Dead end	4.46E+08	1.16E+09	1.14E+09	1.81E+09	7.57E+08	1.81E+09	2.84E+09	4.11E+09
Cross-fLow	ND	1.72E+09	ND	4.14E+09	ND	3.18E+08	ND	3.28E+09

ND: Not determined